Anatomically weighted 2nd order Total Variation reconstruction of ^{23}Na MRI using ^{1}H prior information

Christine Gnahm[1], Nicolas G.R. Behl[1], Armin Biller[2], Peter Bachert[1], and Armin M. Nagel[1]

[1]*Medical Physics in Radiology, German Cancer Research Center (DKFZ), Heidelberg, Germany,* [2]*Department of Neuroradiology, University Hospital Heidelberg, Heidelberg, Germany*

Purpose

^{23}Na MRI provides functional information about cell viability that may become clinically relevant for diseases such as stroke, cancer or multiple sclerosis (MS)(1). However, it is still hampered by low signal-to-noise ratio (SNR) and long acquisition times. By using iterative reconstruction methods, noise and artifact level can be reduced. Recently, it was shown that even the minimal anatomical information contained in a binary mask of the brain used as support constraint is beneficial in combination with a Total Variation (TV) constraint (2). Here, we present a new regularization that uses more sophisticated anatomical a priori information from ^{1}H MRI. We exploit the fact that prominent anatomical features are visible in images from both nuclei. Through anatomical weighting of the TV constraint, intensity variations in the ^{23}Na image are promoted at positions of known tissue boundaries. The method is evaluated through simulations and MR examinations of a MS patient.

Methods

a) Iterative image reconstruction with anatomically weighted 2nd order TV regularization (AnaWeTV)

Image reconstruction is formulated as constrained optimization problem with a support constraint as described in (2). A priori information from ^{1}H MRI is incorporated through anatomically weighted 2nd order TV regularization (AnaWeTV). The weighting factors express the confidence of intensity variations between adjacent voxels (3, Fig. 1d). We use a 2nd order TV regularization that - in contrast to the patchy images created by 1st order TV - allows for a correct reconstruction of signal intensity gradients while preserving edge structures (4, 5). The regularization term calculated for the image vector ρ is

$R(\rho) = \sum_{\alpha=x,y,z} \left(\lambda \left\| W_\alpha D_\alpha^{(1)} \rho \right\|_1 + (1-\lambda) \left\| W_\alpha D_\alpha^{(2)} \rho \right\|_1 \right)$, with relative weighting $\lambda = 0.77$ (4). $D_\alpha^{(1)}$ denotes the 1st order derivative computing the finite differences in dimension α, and $D_\alpha^{(2)} = D_\alpha^{(1)T} D_\alpha^{(1)}$ is the 2nd order derivative. W_α is a diagonal matrix containing anatomical information in form of weighting factors, which are calculated directly from a registered high-SNR, high-resolution ^{1}H MR reference image normalized to its maximum value. W_α is calculated from the inverse w_α of the confidence c_α of tissue boundary, which we define as the finite differences of the reference image r: $(W_\alpha)_{ii} = 0.1 \cdot (w_{\alpha,i} - \min(w_\alpha))(w_{\max} - \min(w_\alpha))^{-1}$ for $w_{\alpha,i} < w_{\max}$ and $(W_\alpha)_{ii} = 1$ for $w_{\alpha,i} = w_{\max}$; with $w_{\alpha,i} = \min\{(c_{\alpha,i})^{-1}, w_{\max}\}$ and $c_{\alpha,i} = \left(D_\alpha^{(1)} r\right)_i$. The parameter $w_{\max}$ controls which signal variations in the reference are included as prior information. For small values of $w_{\max}$, only the strongest borders contribute.

b) Simulated brain with MS lesions and MR measurements

Image reconstruction was simulated for T_2-weighted ^{1}H MRI of a brain with MS lesions from the BrainWeb database (2, 6). The dataset was generated with the same parameters as the ^{23}Na measurement (see below). The ^{1}H image with resolution (1.5 mm)³ was used as reference for weighting factor calculation (Fig. 1a & 1d). A ^{23}Na dataset of the brain of a MS patient was acquired on a 7 T whole body system (Magnetom 7 T, Siemens Healthcare, Erlangen, Germany) using a double-resonant (^{1}H: 297.2 MHz; ^{23}Na: 78.6 MHz) quadrature birdcage coil (Rapid Biomed GmbH, Rimpar, Germany). A density-adapted 3D radial projection pulse sequence (7) with 25 % of the required Nyquist projections was applied (TE / TR = 0.3 / 120 ms; readout time = 10 ms; α = 90°; nominal resolution = (3 mm)³; projections = 5k; T_{AQ} = 10 min). The measurement was performed with the approval of the ethics committee Heidelberg. Anatomical ^{1}H images were acquired as part of the clinical routine protocol on a 3 T MR system (Magnetom Tim Trio, Siemens Healthcare, Erlangen, Germany). The weighting factors were calculated from a T_1-weighted MPRAGE image (Fig. 2a; TE / TR = 3.42 / 1740 ms; BW = 180 Hz/px; α = 15°; nominal resolution = (1 mm)³; T_{AQ} = 3 min 43 sec). The images were registered using the FLIRT tool of the FSL library (8).

c) Reconstruction evaluation

Root mean square error (RMSE) and structural similarity (SSIM, 9) were calculated within the support region for the simulation results. Optimal weighting factors for the regularization terms were determined in a parameter study analyzing RMSE, SSIM and artifact level for a range of parameter pairs. The accuracy of reconstructed intensities was evaluated in four small MS lesions (arrows in Fig. 1) by comparing the mean signal within each lesion to the ground truth. The mean deviation (MD) for the 4 lesions was calculated. SNR maps were obtained using the pseudo multiple replica method with 100 replicas (10) for all reconstructions.

Results

The AnaWeTV reconstruction enhances resolution of known tissue borders in the low-resolution ^{23}Na image. Thus, partial volume effects are reduced (Fig. 1c & 2c). In simulated data, the RMSE decreases by 44% and the SSIM increases by 32% compared to gridding (Table 1). The intensity of MS lesions, whose boundaries are included in the anatomical weighting, is reconstructed more accurately (MD = 2.8%) than with gridding (MD = 6.9%). SNR is increased compared to gridding by a factor of 2.0 in the cerebral spinal fluid (CSF) of the lateral ventricles and 3.8 in white matter (WM). For in vivo ^{23}Na MRI of the brain of a MS patient, small CSF structures that are very noisy in the gridding images (Fig. 2b$_1$) are depicted clearly in the AnaWeTV images (Fig. 2c$_1$). Large and small MS lesions are well visible (arrows in Fig. 2c$_2$). Here, we obtain an SNR which is 2.2 times higher in CSF and 1.6 times higher in WM compared to gridding.

Discussion

In the proposed AnaWeTV reconstruction, features not contained in the weighting factors are reconstructed with a conventional 2nd order TV regularization. This means less blurring than in method of reference 3, where quadratic regularization is used. The total sodium concentration in small structures that are known a priori can be determined more precisely. Thus, the AnaWeTV algorithm is in particular beneficial for the assessment of tissue structures that are visible in both ^{23}Na and ^{1}H MRI.

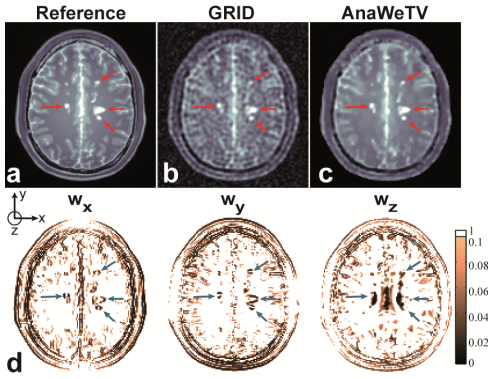

Fig. 1: *Simulated images of a brain with MS lesions. a) Reference image used as ground truth. b) Gridding and c) AnaWeTV reconstruction. d) Weighting factors used in the AnaWeTV reconstruction with parameter w_{max}=20 controlling the extent of included prior information. Arrows mark four MS lesions used to evaluate the accuracy of reconstructed intensities.*

Table 1*: Calculated RMSE, SSIM, MD and SNR values for the reconstructed images*

		GRID	AnaWeTV
Simulation	RMSE	0.27	0.15
	SSIM	0.57	0.75
	MD	6.9%	2.8%
	SNR, WM	9.5	35.7
	SNR, CSF	22.6	45.0
MS patient	SNR, WM	6.2	13.5
	SNR, CSF	21.8	35.5

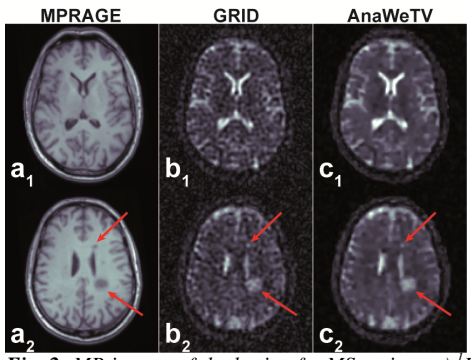

Fig. 2: *MR images of the brain of a MS patient. a) ^{1}H image used for weight calculation. b) & c) ^{23}Na MR images of the same patient reconstructed with b) gridding and c) AnaWeTV (w_{max} = 30). The arrows mark two MS lesions.*

Reference

1. Madelin and Regatte, J Magn Reson Imag (2013) 38, 511. **2.** Gnahm et al., Magn Reson Imag (2013) doi:10.1002/mrm.24827 **3.** Haldar et al., Magn Reson Med (2008) 59, 810. **4.** Geman et al., IEEE T Med Imag (1995) 4, 932. **5.** Block et al., Magn Reson Med (2007) 57, 1086. **6.** Cocosco et al., NeuroImage (1997) 5, 425. **7.** Nagel et al., Magn Reson Med (2009) 62, 1565. **8.** Jenkinson et al., Med Image Anal (2001) 5(2),143. **9.** Wang et al., IEEE T Image Process (2004) 13(1), 600. **10.** Robson et al., Magn Reson Med (2008) 60, 895.